International Journal of Machine Tools & Manufacture 56 (2012) 28–38

Contents lists available at SciVerse ScienceDirect

International Journal of Machine Tools & Manufacture

journal homepage: www.elsevier.com/locate/ijmactool

Chatter modelling in micro-milling by considering process nonlinearities

S.M. Afazov *, S.M. Ratchev, J. Segal, A.A. Popov

Manufacturing Research Division, University of Nottingham, Nottingham NG7 2RD, UK

ARTICLE INFO

Article history:
Received 19 September 2011
Received in revised form
19 December 2011
Accepted 20 December 2011
Available online 3 January 2012

Keywords:
Micro-milling
Chatter
Stability lobes
Cutting forces
Run-out
Cutting tool dynamics

ABSTRACT

This paper presents a new approach for chatter modelling in micro-milling. The model takes into account: the nonlinearity of the uncut chip thickness including the run-out effect; velocity dependent micro-milling cutting forces; the dynamics of the tool-holder-spindle assembly. The uncut chip thickness is determined after considering the full kinematics of the cutting tool including the run-out effect. The micro-milling cutting forces are determined by: (i) a finite element (FE) prediction of the cutting forces in orthogonal cutting at different cutting velocities and uncut chip thicknesses; (ii) describing the relationship between cutting forces, cutting velocities and uncut chip thicknesses into a nonlinear equation; (iii) incorporating the uncut chip thickness model into the relationship of the cutting forces as function of the cutting velocity and the uncut chip thickness. The modal dynamic parameters at the cutting tool tip are determined for the tool-holder-spindle assembly and used for solving the equation of motion. The micro-milling process is modelled as two degrees of freedom system where the modal dynamic parameters for the tool-holder-spindle assembly and the micro-milling cutting forces are considered. Due to nonlinearities in the micro-milling cutting forces, the equation of motion is integrated numerically in the time domain using the Runge–Kutta fourth order method. The displacements in the x and y directions are obtained for one revolution-per-tool. Statistical variances are then employed as a chatter detection criterion in the time-domain solution. Scanning electron microscope (SEM) inspection is carried out to observe potential chatter marks on the micro-milled AISI 4340 steel surfaces at different spindle speeds and depths of cut. The predicted stability lobes and the experimentally obtained stability limits resulted in satisfactory agreement. The influence of the run-out effect on the stability lobes at different feed rates was investigated, which demonstrated the capability of the developed chatter model to consider quantitatively the run-out phenomenon. The results showed that the stability limits decrease by increasing the run-out length.

1. Introduction

Chatter is a self-excited vibration between a cutting tool and a workpiece in conventional milling or micro-milling. It is characterised by poor surface quality and fast tool wear. Cutting tool damage and reduced material removal rate can also be observed. The negative effects caused by chatter have encouraged researchers in the last six decades to develop different theories and models for predicting and preventing this phenomenon. Most of the developed theories and models are applied to conventional milling. Due to the recent industrial demands for miniaturised components, the micro-milling process has widened its usability for producing micro-parts and features. This has demanded the development of new models and techniques for chatter modelling in micro-milling.

A selected number of recently published papers are presented to highlight the recent developments in chatter. Altintas et al. [1] have compared chatter models with multi-frequency solutions [2,3] and semi-discrete time domain solution [4–6]. The comparison between and advantages of the two models have been described for simple examples in conventional milling. Sims et al. [7] have investigated three solutions for predicting the stability of variable pitch or helical milling tools. The first is a semi-discretisation formulation that performs spatial and temporal discretisation of the tool. The second is a time-averaged semi-discretisation formulation that assumes time-averaged cutting force coefficients. The third is a temporal finite element formulation that can predict the stability of variable pitch tools with a constant uniform helix angle, at low radial immersion. Quintana et al. [8] have presented an experimental method for identifying the stability diagram lobes in conventional milling. The cutting trials have been performed on a workpiece with an inclined surface where the axial depth of cut gradually increases. Chatter is detected by recording and analysing the sound amplitudes and frequencies. Kuljanic at al. [9] researched the application of several different types of sensors and methodologies for chatter detection in face milling in order to determine, which

* Corresponding author.
E-mail address: shukri.afazov@nottingham.ac.uk (S.M. Afazov).

0890-6955
doi:10.1016/j.ijmachtools.2011.12.010

sensor type or which combination of sensors is more suitable for industrial applications. They have found that the multisensor combinations of three or four sensors are strongly recommended, since it is possible to achieve high levels of accuracy and robustness. Rahnama et al. [10] have extended the work carried out by Tobias [11], Opitz [12] and Tlusty [13] on conventional chatter by incorporating process damping to predict the chatter stability lobes in micro-milling. The process damping parameters have been obtained using the equivalent volume interface between the tool and the workpiece. They have performed experimental cutting trials to detect the chatter. The occurrence of chatter has been examined using an acoustic emission (AE) sensor. They have also observed that chatter causes burr formation. Sims et al. [14] have investigated the chatter stability of milling processes using a fuzzy logic algorithm in order to accommodate uncertainty or variability in the model input parameters. A design of experiments approach to implement fuzzy arithmetic has been developed. It has been shown that this formulation is suitable for the chatter prediction problem, particular for the more straightforward time-averaged chatter model.

In micro-milling, material removal is achieved mainly with the cutting tool edge. Depending on the size of the cutting tool edge radius and the applied feed rate, the material can be removed in the form of chips or just ploughed without forming a chip. The boundary between these two phenomena is known as a minimum chip thickness, which depends on the size of the edge radius, feed rate, workpiece material, cutting velocity, tool-workpiece interface friction, etc. Typically, the tool edge radius is not considered in conventional milling while in micro-milling it has a major influence on the process. Also, the run-out phenomenon in micro-milling has significant influence on the cutting forces and surface finish. Recently, Afazov et al. [15] have developed a model, which considers the nonlinearity of the cutting forces and the uncut chip thickness by considering the run-out effect. The nonlinearity of the cutting forces, mainly caused by the cutting tool edge and the velocity dependency, is described by a nonlinear equation proposed by the authors.

Despite the large volume of research conducted in chatter modelling and characterisation of conventional machining in the last six decades, there are still knowledge gaps in micro-milling chatter modelling, especially considering the nonlinearities of the micro-milling process. The objectives of this paper are to develop a new chatter model in micro-milling, which incorporates: the full kinematics of the cutting tool including the run-out effect; nonlinearities due to velocity dependant, ploughing and shear dominant cutting forces on micro-scale and modal dynamic parameters of the tool-holder-spindle assembly; and, a chatter criterion in time domain solution using statistical variances. Another aim is to inspect the surface finish using scanning electron microscope (SEM) for chatter marks at different spindle speeds and cutting depths and find a correlation between the surface finish and the theoretical chatter model and validate the model. Investigation of the run-out effect on the stability lobes in micro-milling is also aimed to provide new knowledge in the field.

The objectives of this study are approached following the methodology in Section 2. First, the authors' developed model [15] for prediction of micro-milling forces, considering the nonlinear cutting forces from FE model of orthogonal cutting and the run-out effect is used in this study. The actual model and results for AISI 4340 steel are presented in Section 3. An approach for determining the modal dynamic parameter for the tool-holder-assembly system is shown in Section 4. After determining the cutting forces and the modal dynamic parameters, the equations of motion described for a two degree of freedom (2DOF) micro-milling system are solved numerically in the time domain to obtain the displacements in the x and y directions. A stability lobes diagram is obtained after employing the statistical variances method as a chatter detection criterion (see Section 5). SEM inspection for chatter marks is performed on micro-milled surfaces at different spindle speeds and depths of cut and the results are compared with the proposed theoretical chatter model in Section 6. Finally, the influence of the run-out effect is investigated at different feed rates in Section 7.

2. Methodology

The methodology in this study (see Fig. 1) includes modelling and prediction of micro-milling cutting force, experimental programme for validation of the modelled and predicted cutting forces, modelling the modal dynamic parameters at the cutting tool tip of the tool-holder-spindle assembly, chatter modelling in time domain solution and experimental programme for validation of the chatter model. The research is specifically focused on chatter modelling, which considers the nonlinearities of the micro-milling process, such as: run-out effect; velocity dependent cutting forces; effect of the cutting tool edge radius on the ploughing and shear dominant cutting forces. The micro-milling cutting forces are identified using the approach developed by Afazov et al. [15]. The approach consist of three models (see Stage 1 from Fig. 1): uncut chip thickness model, FE model of orthogonal cutting, and integrated micro-milling cutting force model. The uncut chip thickness model considers the full kinematics of the cutting tool including the run-out effect. The FE model of orthogonal cutting predicts the cutting forces for specified cutting conditions and cutting tool geometries, especially the cutting tool edge radius, which plays a significant role in micro-milling. The integrated micro-milling cutting force model incorporates the results obtained from the uncut chip thickness model and the FE model of orthogonal cutting where the cutting forces are determined in the x and y directions. An experimental programme is conducted to validate the modelled cutting forces (see Stage 2 from Fig. 1) [15]. The modal dynamic parameters at the cutting tool tip considering the tool-holder-assembly dynamics are obtained in the model presented in Stage 3 from Fig. 1. This model is based on the receptance coupling technique where the frequency response function (FRF) is determined and the model dynamic parameters are obtained using curve fitting methods. The FRF determined by Malekian et al. [16] are used in this study. The chatter model in time domain solution is developed and the inputs from the micro-milling cutting force model and the tool-holder-spindle dynamics model are incorporated into the equations of body motion of 2DOF micro-milling system. The equations of body motion are integrated numerically to obtain the displacements in the x and y directions. Statistical variances are then employed as criterion for chatter detection. An experimental programme is conducted to validate the stability lobes predicted from the proposed chatter model (see Stage 5 from Fig. 1).

3. Cutting force modelling

The micro-milling cutting forces model developed by the authors is used in the current study [15]. This model consists of a mathematical model, which determines the uncut chip thickness in the presence of the run-out effect and FE model, which predicts the relationship between cutting forces, uncut chip thickness and cutting velocities. The two models are then integrated to obtain the micro-milling cutting forces. Furthermore, this approach has been used for predicting the cutting forces for AISI H13 steel [17] and Ti6Al4V alloy [18] where very good agreement between predicted and experimentally measured

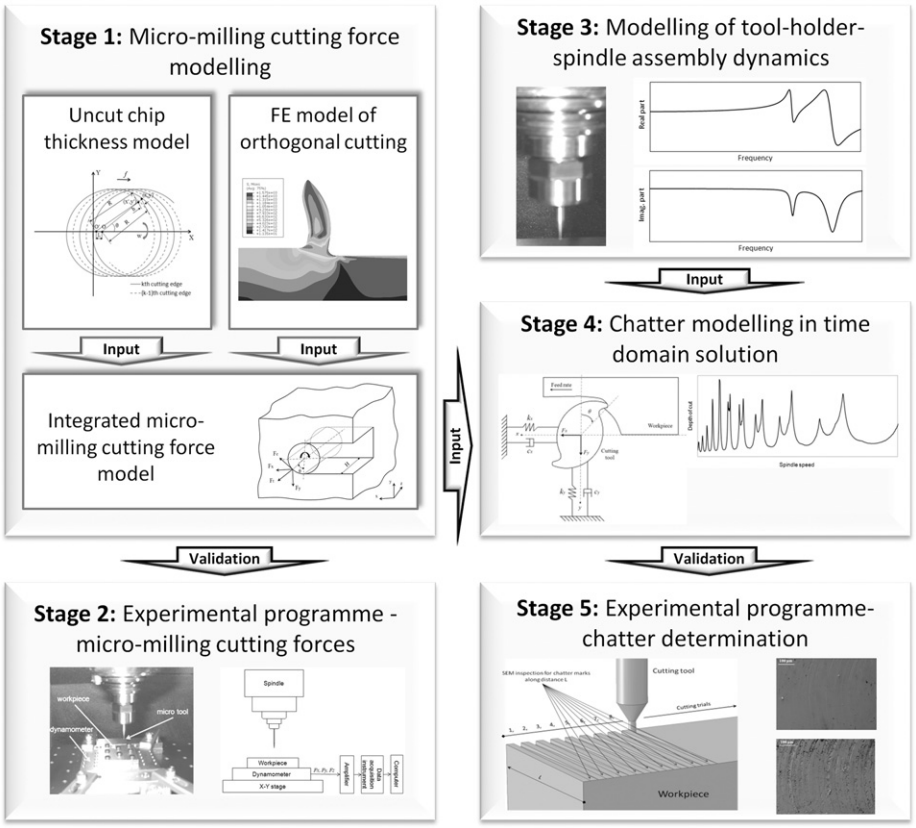

Fig. 1. Methodology diagram.

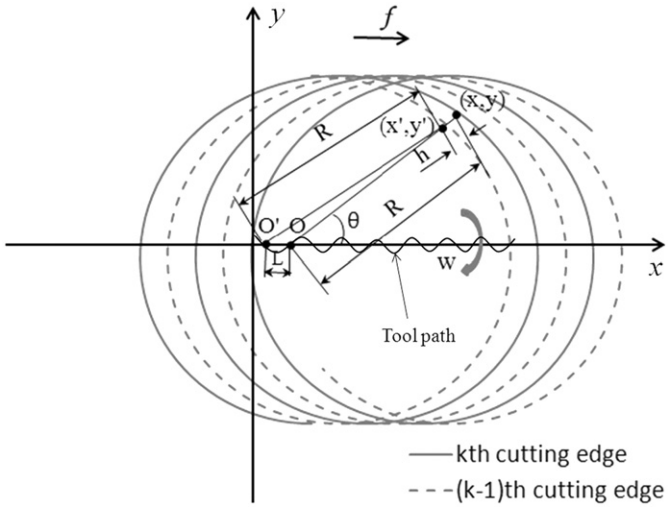

Fig. 2. Trajectory of the k^{th} and the $(k-1)^{th}$ tool edges in the x–y Cartesian coordinate system.

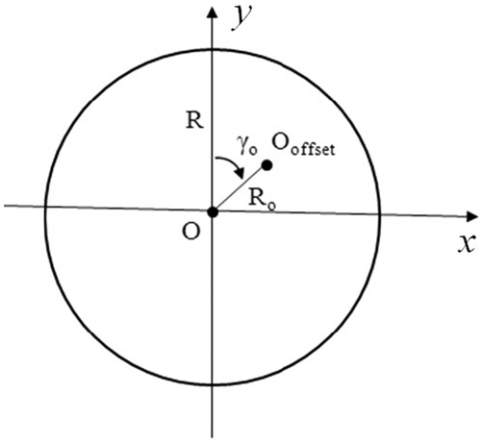

Fig. 3. Cutting tool centre offset.

cutting forces has been achieved for both materials. Also, Jin and Altintas [19] predicted and validated the micro-milling cutting forces using FE model of orthogonal cutting for Brass 260. A brief description of the model and main results are presented in this section.

3.1. Uncut chip thickness model

The trajectory of the tool edge depends on the radius of the tool, spindle angular velocity, run-out effect and the feed rate. Fig. 2 shows the trajectory of the k^{th} and the $(k-1)^{th}$ edges of the tool. Radial run-out or eccentricity of the cutting tool is a common problem in the micro-milling process. The main source of run-out is the cutting tool centre offset (see Fig. 3). As reported by Bao and Tansel [20], a small run-out creates significant force variations in micro-milling.

The trajectory of the k^{th} edge can be given as

$$x_{(k)} = ft + R\sin(wt - 2\pi k/K) + R_o\sin(wt + \gamma_0)$$
$$y_{(k)} = R\cos(wt - 2\pi k/K) + R_o\cos(wt + \gamma_0) \quad (1)$$

where f is the feed rate (mm/s), R is the radius of the tool (mm), w is the spindle angular velocity (rad/s), t is the time (s), k is the flute number, K is the number of flutes, R_o is the run-out length (mm), γ_0 is the run-out angle (rad). The trajectory of the $(k-1)^{th}$

cutting edge can be defined from Eq. (1) by replacing k with $(k-1)$ and t with t'

$$x_{(k-1)} = ft' + R\sin(wt' - 2\pi(k-1)/K) + R_o\sin(wt' + \gamma_o)$$
$$y_{(k-1)} = R\cos(wt' - 2\pi(k-1)/K) + R_o\cos(wt' + \gamma_o) \quad (2)$$

The time t', representing the time of the $(k-1)^{th}$ cutting edge, can be defined by expressing R for Eqs. (1) and (2) and then substituting them to form Eq. (3), which is solved numerically using the Newton–Raphson method:

$$R\tan(wt-2\pi k/K)\cos(wt'-2\pi(k-1)/K) + R_o\tan(wt-2\pi k/K)\cos(wt'+\gamma_o)$$
$$-R_o\tan(wt-2\pi k/K)\cos(wt+\gamma_o) - ft' + ft - R\sin(wt'-2\pi(k-1)/K)$$
$$-R_o\sin(wt'+\gamma_o) + R_o\sin(wt+\gamma_o) = 0 \quad (3)$$

From the geometric relationship, the uncut chip thickness h (mm) can be given by

$$h = R + L\sin(wt - 2\pi k/K + \alpha_o) - \sqrt{R^2 - L^2\cos^2(wt - 2\pi k/K + \alpha_o)} \quad (4)$$

where the distance L and the angle α_o are:

$$L = \sqrt{(x_o - x_{o'})^2 + (y_o - y_{o'})^2} \quad (5)$$

$$\alpha_o = \arctan\left(\frac{y_o - y_{o'}}{x_o - x_{o'}}\right) \quad (6)$$

The coordinates of nodes O and O′ are:

$$x_{(O)} = ft + R_o\sin(wt + \gamma_o)$$
$$y_{(O)} = R_o\cos(wt + \gamma_o) \quad (7)$$

$$x_{(O')} = ft' + R_o\sin(wt' + \gamma_o)$$
$$y_{(O')} = R_o\cos(wt' + \gamma_o). \quad (8)$$

3.2. FE model of orthogonal cutting

The FE model of orthogonal cutting (see Fig. 4) shows the tool-workpiece interaction, geometrical parameters and material removal in the form of a chip. Finite element analyses (FEA) are performed in dynamic fully coupled thermo-mechanical FE code using explicit integration for solving the equation of motion in ABAQUS/Explicit [21]. Explicit FE code is used to avoid conversion problems due to the high deformation rates involved in micro-milling cutting processes. Small time increments are required in modelling the high deformation rates induced in micro-milling. Since small time increments are required, the accuracy of the explicit integration method is satisfactory. Also, the computational time is shorter compared to the implicit integration method, which requires solving numerically nonlinear equations with the iterative Norton–Raphson method [22]. In the current FE model, the tool moves into the workpiece with velocity (v) and uncut chip thickness (h). Due to the small size of the tool, the tool edge radius is defined using SEM measurements. The edge shape of the tool is approximated as a radius (r) of 3.5 μm. The rake angle (α) and the clearance angle (γ) are 8° and 40°, respectively. The tool is modelled as rigid body represented by a reference point (RP). Plane strain conditions are used within the FEA. The workpiece is modelled as a rectangular block and meshed with four node bilinear temperature-displacement elements with reduced integration and hourglass control. Generally, the elements thickness in plain strain FEA can be used to represent the depth of cut in milling. Elements thickness (a_p^{orth}) of 1 mm is applied to the model, which is used as a reference when different depths of cut are investigated. An inelastic heat fraction is used in the model where 90% of the plastic work is converted into heat. Also, the heat generation due to the contact between the workpiece and the tool is considered. The fraction of dissipated energy converted into heat is assumed to be 100% and the heat is distributed equally between the two surfaces in contact. Arbitrary Lagrangian Eulerian (ALE) adaptive meshing is used to avoid element distortions due to the high deformation rates. A slip-stick friction model is applied between the tool and the workpiece. It should be mentioned that the friction contributes for the nonlinearities of the cutting forces since the contact pressure varies across the contact length between the tool and the workpiece. For example, the edge radius creates higher contact pressure where the friction results in a sticking-dominant behaviour.

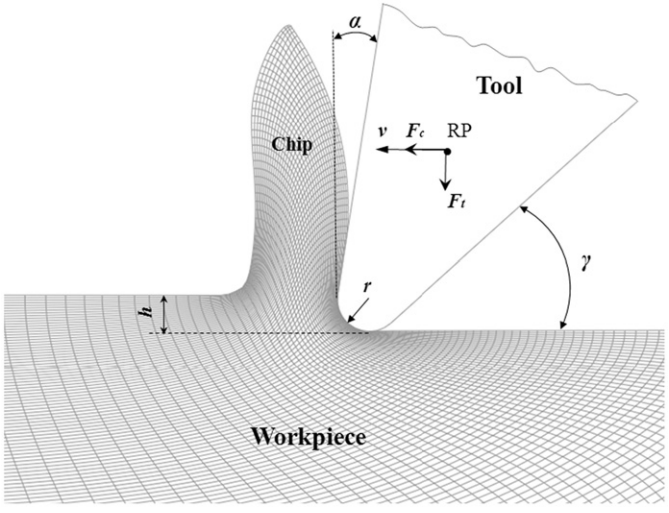

Fig. 4. Schematic of FE orthogonal cutting process.

AISI 4340 steel is employed and the workpiece is modelled as an isotropic thermal-elastic-plastic model using the Johnson–Cook constitutive equation. The model is a strain-rate and temperature dependent visco-plastic material model

$$\sigma = (A + B\bar{\varepsilon}^n) \times \left[1 + C\ln\left(\frac{\dot{\bar{\varepsilon}}}{\dot{\bar{\varepsilon}}_0}\right)\right] \times \left[1 - \left(\frac{T - T_r}{T_{melt} - T_r}\right)^m\right] \quad (9)$$

where $\bar{\varepsilon}$ is the equivalent plastic strain, $\dot{\bar{\varepsilon}}$ is the plastic strain rate, $\dot{\bar{\varepsilon}}_0$ is the reference strain rate (1 s^{-1}), T is the reference temperature, T_r is the transition or room temperature, T_{melt} is the melting temperature, A is the initial yield stress, B is the hardening modulus, n is the hardening exponent, C is the strain rate dependency coefficient and m is the thermal softening coefficient. Full details for the FE model, applied loads, thermal and mechanical boundary conditions can be found in [15], together with all parameter values.

An important feature of the micro-milling process is the presence of size-effect or dependence of strength on the scale of deformation as observed by a number of researchers. This is mainly due to the material behaviour at micro-scale since the feed rates in micro-milling are comparable with the material grain sizes. Generally, the size-effect can be described as a nonlinear increase of the specific cutting energy at different micro-machining cutting conditions. The size-effect can be explained by: (i) the decreasing number of defects in microstructure, (ii) the increasing strain rate at the primary shear zone, (iii) the effect of thermal softening and (iv) the effect of strain gradient plasticity at the deformation zones at low uncut chip thickness and (v) the effect of the negative rake angle generated by the edge radius. In relation to the size-effect phenomenon, Afazov et al. [18] considered the size-effect in determining the micro-milling cutting forces of Ti6Al4V alloy by modelling the material stress flow using the Johnson–Cook constitutive material model and the strain gradient plasticity theory. It has been observed that the material model using the strain gradient

plasticity results in a better correlation with the experimentally obtained micro-milling cutting forces for feed rates less or equal to 6 μm/tooth, while the Johnson–Cook material model predicts more accurately the micro-milling cutting forces for feed rates of 12 μm/tooth. In relation to material modelling and size-effect, it has been also observed that the Johnson–Cook constitutive material model results in a good correlation between experimental and predicted micro-milling cutting forces for AISI H13 steel with the enhancement that the material hardness is considered in the constitutive material model [17].

3.3. Integrated model—results and validation

The relationship between the cutting forces and the uncut chip thickness at different cutting velocities is obtained using the FE model and the results are shown in Fig. 5. It can be seen that the forces in the cutting direction decrease with increasing the velocity. This is mainly due to the material softening at high velocities where the temperature increases and the inertia effects, taken into account in the dynamic FEA. The forces in the tangential direction can be assumed velocity independent. The effect of the edge radius on the nonlinearity of the cutting forces can be seen in Fig. 5 for small uncut chip thicknesses. It is also true that by increasing the edge radius due to wear, the nonlinearities of the cutting forces increase for higher uncut chip thicknesses as discussed in [23].

The relation between the uncut chip thickness and the cutting forces for each velocity can be given by a two-phase exponential equation:

$$F_{c,t} = d_1\left[1-\exp(d_2 h)\right] + d_3\left[1-\exp(d_4 h)\right] \tag{10}$$

After determining the constants (d_1, d_2, d_3 and d_4) from Eq. (10), it was observed that the constants d_1 and d_3 are velocity dependent while d_2 and d_4 were constant. The constants d_1 and d_3 were plotted versus the velocity (v). It was observed that the relations between $d_1 - v$ and $d_3 - v$ can be described by exponential and linear functions, respectively. Eq. (11) shows the full relation between cutting forces, uncut chip thickness and velocity:

$$F_{c,t} = (p_1 v^{p_2})[1-\exp(p_3 h)] + (p_4 v + p_5)[1-\exp(p_6 h)] \tag{11}$$

The cutting velocity from the orthogonal cutting model can be represented as a tangential velocity of the cutting tool and can be given by

$$v = w(R - 0.5h \times 10^{-3}) \tag{12}$$

It must be noted that the unit of the uncut chip thickness (h) in Eqs. (11) and (12) is μm. The constants for Eq. (11) are obtained and the fitted curves are shown in Fig. 5. The constants are given in Table 1.

The micro-milling cutting forces in the cutting and tangential directions can be determined by substituting Eqs. (4) and (12) into Eq. (11). The micro-milling forces in the x and y directions can be given by

$$\begin{bmatrix} F_x \\ F_y \end{bmatrix} = \frac{a_p}{a_p^{orth}} \begin{bmatrix} \sin\theta & \cos\theta \\ -\cos\theta & \sin\theta \end{bmatrix} \begin{bmatrix} F_t \\ F_c \end{bmatrix} \tag{13}$$

where a_p is the depth of cut (0.1 mm at the current validation study), a_p^{orth} is the element thickness from the orthogonal FE model (1 mm at the current study) and θ is the angle of rotation. Validated results of three selected cutting conditions are shown in Figs. 6–8. It can be seen that the modelled and experimental cutting forces result in very good correlation. The run-out effect on the cutting forces can be also seen where the cutting forces for the second tooth are lower, which can be correlated to micro-milling nonlinearity, since the chatter model presented in Section 5 considers a full revolution of the cutting tool. This is because the run-out results in different uncut chip thicknesses for the two teeth. More validated results for 8 cutting conditions can be found in [15]. The presented approach for obtaining the cutting constants does not require experimental tests. The experimental tests are only used for validation of the micro-milling cutting forces.

It is also worth mentioning that the FE model of orthogonal cutting is capable to predict the cutting temperature. The results have shown that the maximum temperature located near the tool-chip interface increases by increasing the uncut chip thickness and the cutting velocity [15]. In relation to the current study, the cutting temperature affects the cutting forces by softening the material and further the process stability. This effect is considered in the obtained cutting constants and used for predicting the process stability by the chatter model presented in Section 5.

Table 1
Constants for Eq. (11).

Constants	AISI 4340 material	
	F_c	F_t
p_1	24,730	13,200
p_2	−0.066	0
p_3	-1.6×10^{-4}	-0.45×10^{-4}
p_4	-1.98×10^{-4}	0
p_5	6.63	6.5
p_6	−6.9	−12

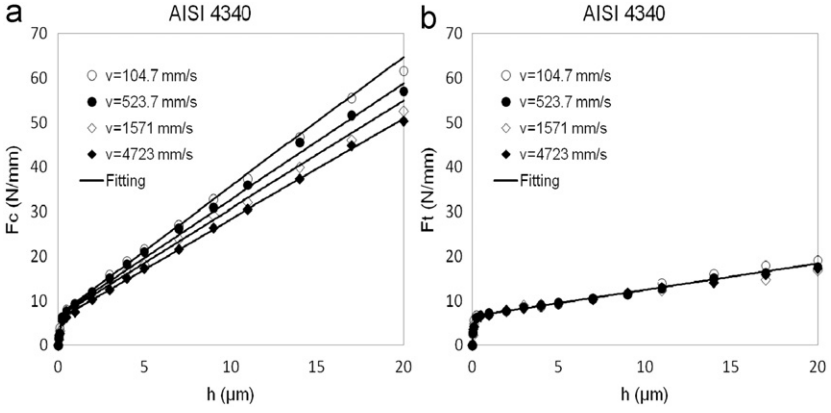

Fig. 5. Cutting forces obtained in: (a) the cutting direction; (b) the tangential direction.

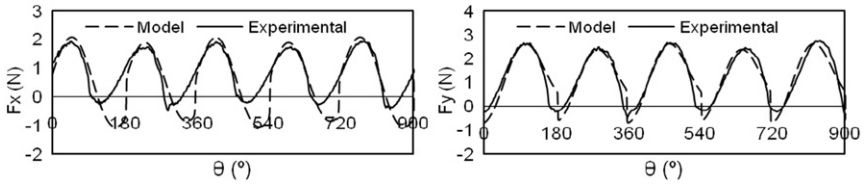

Fig. 6. Forces at w=5000 rev/min and f=1 mm/s; γ_o=45°; R_o=0.3 μm; h_{max}=6.42 μm [15].

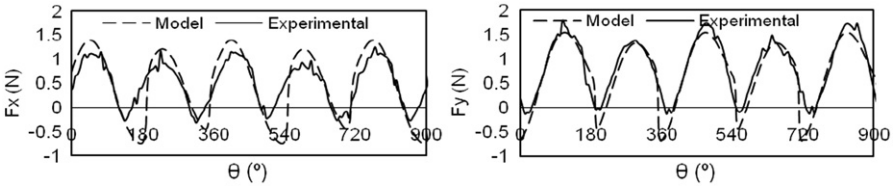

Fig. 7. Forces at w=25,000 rev/min and f=2 mm/s; γ_o=45°; R_o=0.3 μm; h_{max}=2.82 μm [15].

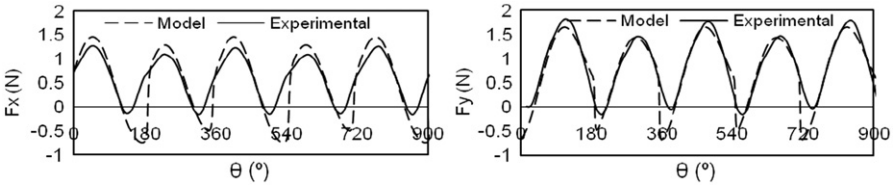

Fig. 8. Forces at w=50,000 rev/min and f=5 mm/s; γ_o=45°; R_o=0.3 μm; h_{max}=3.42 μm [15].

4. Dynamics of the tool-holder-spindle assembly

Typically, the modal dynamics of the tool-holder-spindle assembly in conventional milling is obtained using impact hammer testing where the FRF is determined at the tool tip. Since the micro-milling cutting tools have very small dimensions, accelerometer attachment on the tool tip is extremely difficult, so impact hammer testing cannot be used directly. Melekian at al. [16] have obtained the FRF for the tool-holder-spindle assembly using a receptance coupling technique as follows. The tool-holder-spindle assembly consists of an end-milling carbide cutting tool with diameter of 500 μm attached to a KERN milling machine. The tool-holder-spindle assembly has been divided into two substructures (Substructure A and Substructure B). Substructure A represents the lower part of the micro-end-mill and Substructure B includes the remaining part of the tool and the spindle. The dynamics of Substructure A is obtained using FEA while the dynamics of Substructure B is determined using miniature impact hammer testing. The assembled FRF has been determined after performing the receptance coupling technique for the two substructures [24]. Fig. 9 shows a representative FRF in the real and imaginary parts where the two lowest frequency mode shapes are considered. Since the same micro-milling cutting tools are used in the experimental programme of this study and in [16] with the small difference that the tool in this study is coated and similar KERN milling machines are utilised, the obtained FRF from [16] is used for determining the modal dynamic parameters.

The modal dynamic parameters are determined using the peak-picking and steepest descent fitting methods. The obtained modal dynamic parameters from both methods are used for determining and comparing the chatter stability lobes. The peak-picking fitting method can be described as follows. The FRF in the real and imaginary parts can be given by [25]

$$\mathrm{Re}\left(\frac{X}{F}\right)=\sum_{i=1}^{n}\frac{1}{k_i}\left(\frac{1-r_i^2}{(1-r_i^2)^2+(2\zeta_i r_i)^2}\right)$$

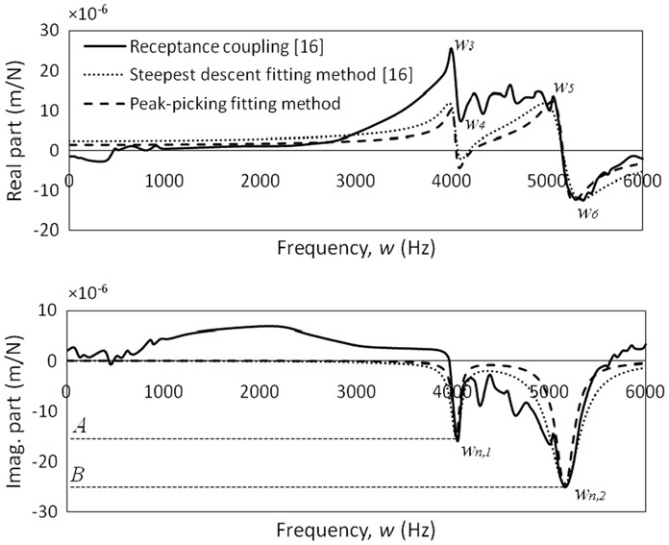

Fig. 9. Representative FRF at the cutting tool tip of the tool-holder-spindle assembly using receptance coupling [16].

$$\mathrm{Im}\left(\frac{X}{F}\right)=\sum_{i=1}^{n}\frac{1}{k_i}\left(\frac{-2\zeta_i r_i}{(1-r_i^2)^2+(2\zeta_i r_i)^2}\right) \tag{14}$$

where n is the number of modes (n=2 for the FRF from Fig. 9), k_i is the modal stiffness of the i^{th} mode, ζ_i is the modal damping ratio of the i^{th} mode, $r_i=w/w_{n,i}$ is the frequency ratio of the i^{th} mode, w is the excitation frequency and $w_{n,i}$ is the modal natural frequency of the i^{th} mode. The frequencies labelled $w_{n,1}$ and $w_{n,2}$ along the frequency axis in the imaginary part of the direct FRF correspond to the minimum imaginary peaks and provide the two natural frequencies. The damping ratios can be given by half-power

Table 2
Modal dynamic parameters for the tool-holder-spindle assembly.

Dynamic modal parameters	First mode shape		Second mode shape	
	Peak-picking fitting method	Steepest descent fitting method [16]	Peak-picking fitting method	Steepest descent fitting method [16]
w_n (Hz)	4035	4035	5163	5163
ζ	0.0105	0.016	0.0216	0.038
k (MN/m)	3.2	2.1425	0.92	0.5397

points:

$$\zeta_1 = \frac{w_4 - w_3}{2w_{n,1}}; \quad \zeta_2 = \frac{w_6 - w_5}{2w_{n,2}} \tag{15}$$

The negative peak values A and B, identified along the vertical axis of the imaginary part of the direct FRF are used to find the modal stiffness values k_1 and k_2, respectively:

$$k_1 = \frac{-1}{2\zeta_1 A}; \quad k_2 = \frac{-1}{2\zeta_2 B} \tag{16}$$

The obtained modal parameters using the peak-picking and steepest descent fitting methods are given in Table 2. Both sets of modal parameters are used in the chatter model where the results are compared. It can be seen that higher modal stiffness and lower modal damping ratio is obtained with the peak-picking fitting method. It is assumed that the dynamics of the cutting tool is the same in the x and y directions due to the tool and spindle cylindrical symmetries.

5. Chatter modelling with time domain solutions

Typically, the chatter is modelled by solving the equation of motion in the frequency or time domain where the cutting forces and modal dynamic parameters at the cutting tool tip are used. The frequency domain solution is mainly used when the milling cutting forces exhibit linear behaviour. This is a typical case in conventional milling. Micro-milling is characterised using cutting tools with small diameters (e.g. diameters between 10 μm and 1 mm) and small feed rates (a few microns per tooth). The micro-milling cutting forces from Fig. 5 show nonlinear behaviour at small uncut chip thicknesses and feed rates, respectively. This nonlinearity of the cutting forces can be explained with the fact that at small uncut chip thicknesses the workpiece material is subjected to ploughing and shearing cutting with chip formation. The boundary between the ploughing and chip formation phenomena is known as a minimum chip thickness, which depends on the size of the cutting tool edge radius, feed rate, workpiece material, cutting velocity, tool-workpiece interaction, etc. The run-out effect and the velocity dependency of the cutting forces also introduce nonlinearities. Since the micro-milling cutting forces are nonlinear, the equation of motion must be solved in the time domain using numerical methods for integrating the ordinary differential equation of motion. By assuming that the helix angle of the micro-milling tool is negligible, the micro-milling system can be reduced to 2-DOF as shown in Fig. 10.

The dynamics of the micro-milling system can be described by two second order ordinary deferential equations for each DOF:

$$\begin{aligned} m_x\ddot{x}(t) + c_x\dot{x}(t) + k_x x(t) &= F_x(v,w,f,a_p,R_o,\gamma_o,t) \\ m_y\ddot{y}(t) + c_y\dot{y}(t) + k_y y(t) &= F_y(v,w,f,a_p,R_o,\gamma_o,t) \end{aligned} \tag{17}$$

In order to incorporate the dynamic modal parameters obtained in Section 4 into the equations of body motion, Eq. (17) is rearranged after dividing with the modal mass and

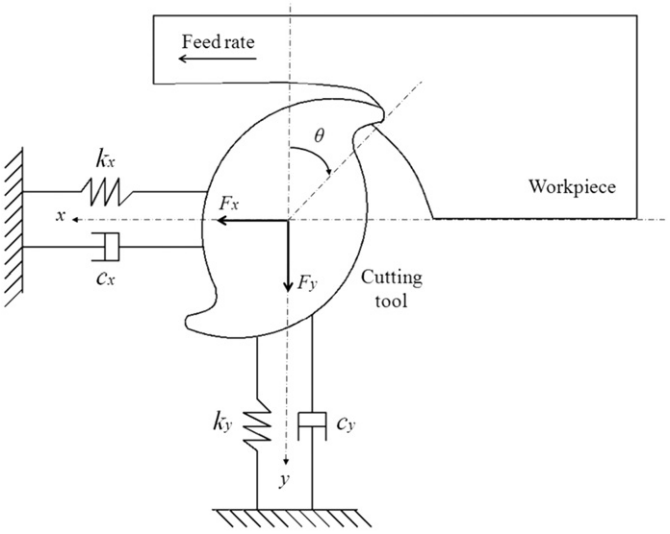

Fig. 10. Dynamic model of micro-milling system.

considering the relationships $c/m = 2\zeta w_n$ and $k/m = w_n^2$ in the form:

$$\begin{aligned} \ddot{x}(t) &= \frac{w_{n,x}^2 F_x}{k_x} - 2\zeta_x w_{n,x}\dot{x}(t) - w_{n,x}^2 x(t) \\ \ddot{y}(t) &= \frac{w_{n,y}^2 F_y}{k_y} - 2\zeta_y w_{n,y}\dot{y}(t) - w_{n,y}^2 y(t) \end{aligned} \tag{18}$$

The fourth order of precision Runge–Kutta numerical integration method is employed to solve Eq. (18) in the time domain solution. The numerical algorithms reported by William et al. [26] are used in the current study. Eq. (18) in the y direction is solved in the same way. Sensitivity analyses are performed to identify the suitable time increment for achieving high accuracy. A time increment $\Delta t = 1 \times 10^{-6}$ s is found to converge with satisfactory accuracy in the current study. After solving Eq. (18) and obtaining the displacements in the x and y directions, the chatter detection criteria is employed. Statistical variances are used as a criterion for detecting the chatter phenomenon in the current chatter model. One revolution-per-tool sampling is used to determine the statistical variances of the predicted displacements in the x and y directions. A sampling of one revolution-per-tool also considers the full run-out effect. The same revolution-per-tool sampling is also used by Schmitz [27] in his study. The statistical variances can be given by [28]

$$s_x^2 = \frac{\sum_{i=1}^{n}(x_i - \bar{x})^2}{n-1}; \quad s_y^2 = \frac{\sum_{i=1}^{n}(y_i - \bar{y})^2}{n-1} \tag{19}$$

where s_x^2 and s_y^2 are statistical variances in the x and y directions, x_i and y_i are the displacements at the corresponding time computed from Eq. (18), n is the number of time increments, $\bar{x}$ and $\bar{y}$ are the averaged displacements in the x and y directions and can be given by

$$\bar{x} = \frac{\sum_{i=1}^{n} x_i}{n}; \quad \bar{y} = \frac{\sum_{i=1}^{n} y_i}{n} \tag{20}$$

Micro-milling cutting is considered unstable when the statistical variances are bigger than the value of 1 μm^2, for example see Zhongqun et al. [29]. A minimum stability limit is considered in this study. The minimum stability limit is determined when one of the statistical variances in the x or y directions has reached 1 μm^2 ($s_x^2 > 1\,\mu m^2$ or $s_y^2 > 1\,\mu m^2$). Fig. 11 shows the block diagram of the actual algorithm for obtaining the stability lobes diagram. It can be seen that the spindle speed is converted from rev/min to

rad/s units and the feed rate for each spindle speed from mm/tooth to mm/s.

Stability lobes at feed rate of 4 μm/tooth are predicted based on the algorithm from Fig. 11 and shown in Fig. 12. The modal dynamic parameters determined from the two fitting methods for the first mode are used as an input. The following incremental initial conditions are used for obtaining the stability lobes in Fig. 12. Spindle speed increment (Δw) of 100 rev/min is used. This means that the stability limits are obtained at every 100 rev/min spindle speed. Selecting smaller Δw can capture better the peak values of the stability lobes but also increase the computational time. From the practical point of view, it is very risky to select stable cutting condition near the peak values of the stability lobes.

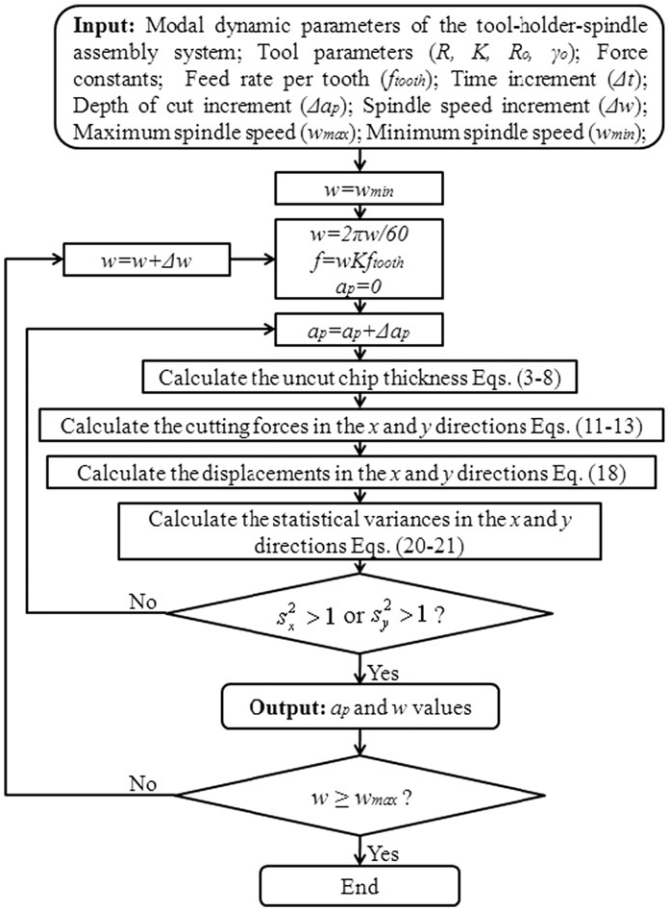

Fig. 11. Block diagram for the algorithm for obtaining the stability lobes in micro-milling.

Therefore, Δw of 100 rev/min is considered a reasonable increment for obtaining the stability lobes in this study. Depth of cut increment (Δa_p) of 1 μm is used. It should also be mentioned that selecting very small Δa_p can provide better accuracy and longer computational time. The stability lobes are obtained in the spindle speed range from 5000 to 100,000 rev/min. The run-out effect is not considered in the predicted stability lobes from Fig. 12 because the aim of these results is to investigate the influence of the modal dynamic parameters. It can be seen that the stability lobes obtained with modal dynamic parameters using the steepest descent fitting have a lower stability limit especially at high spindle speeds. This indicates that the modal dynamic parameters have significant influence on the stability lobes at high spindle speeds. Therefore, the FRF and the modal dynamic parameters must be accurately obtained in order to predict realistic stability lobes. The modal dynamic parameters using steepest descent fitting are used for calculating the stability lobes in the next two sections since lower stability limits are obtained and it is safer for the practitioners to select stable cutting conditions.

6. Experimental programme for inspection of chatter marks using SEM

The experimental methodology and results for chatter marks detection of a micro-milled AISI 4340 steel workpiece is presented in this section. The aim of this experimental study is to relate the obtained results to the stability lobes predicted with the proposed theoretical chatter model. Fig. 13 shows the experimental set-up for performing the cutting trials. The experimental methodology consists of the following sequence: (i) preparation of the workpiece; (ii) clamping the cutting tool to the holder and attaching to the spindle; (iii) measuring the run-out; (iv) performing the cutting trials; (v) inspecting the micro-milled surfaces for chatter marks using SEM.

The AISI 4340 steel workpiece is manufactured with dimensions of 60 mm length, 10 mm width and 10 mm minimum height, and 10.3 mm maximum height, which forms an incline angle of 1.72°. The workpiece is clamped on the stage of the ultra precision 5-axis KERN Evo machine centre. A two-flute TiN coated tungsten tool with diameter of 500 μm and flute length of 1 mm is clamped to the holder and attached to the spindle. The static run-out is measured with a dial indicator attached to the KERN machine centre. Based on the trial-and-error method, the cutting tool has been removed and reattached to the spindle several times until near-zero static run-out is measured on the dial indicator. It is observed that the static run-out is different every time when the cutting tool is clamped to the holder and attached to the spindle, and a static run-out of 4 μm is measured for one of

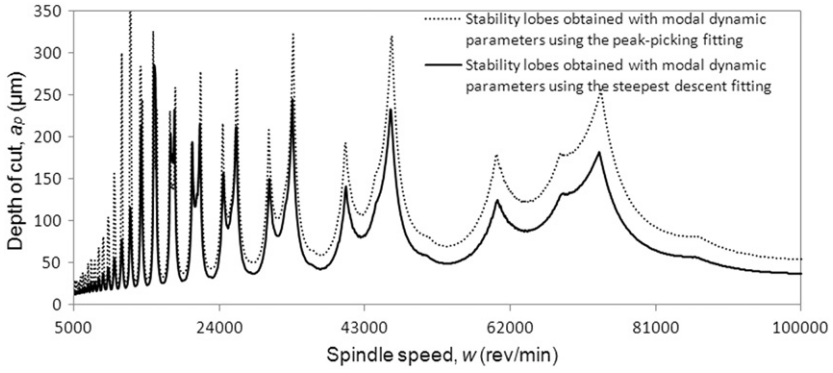

Fig. 12. Stability lobes diagram obtained at 4 μm/tooth feed rate.

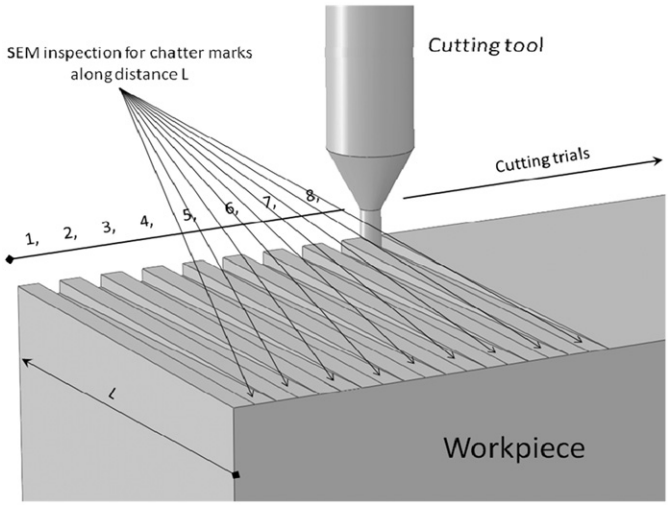

Fig. 13. Experimental set-up and cutting trials.

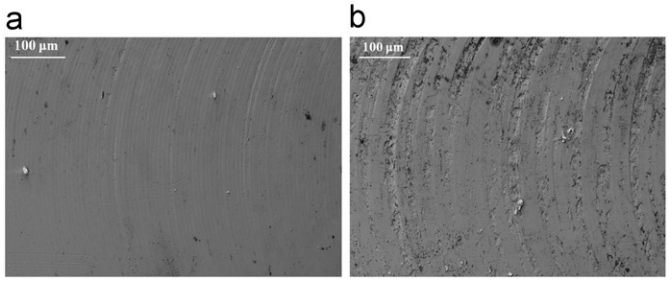

Fig. 14. SEM images of regions with: (a) no chatter marks; (b) chatter marks.

the cases. For instance, a run-out of 4 μm can have a significant impact on the micro-milling cutting forces and stability lobes. The run-out measurements indicated that the cutting tool clamping to the holder has significant effect on the static run-out. Similar to Quintana et al. [8], the cutting trials are performed on a workpiece with inclined surface where the axial depth of cut gradually increases from 0 to 300 μm. The inclined workpiece surface is designed based on the predicted stability lobes from Fig. 12 with maximum of 300 μm depth of cut. The cutting tool moves along the distance L by starting from zero depth of cut and reaching 300 μm at the end of distance L. Forty one cutting trials are performed from 10,000 to 50,000 rev/min spindle speeds with increment of 1000 rev/min and constant feed rate of 4 μm/tooth. SEM inspection with commercially available SEM/FIB CrossBeam workstation (NVision 40: Carl Zeiss SMT) is performed on the micro-milled surfaces along a distance L to investigate the surface finish for potential chatter marks.

Fig. 14 shows SEM images with smooth and rough surface finish obtained at spindle speed of 10,000 rev/min. The image with the smooth surface finish is captured at very small depths of cut where no chatter is expected. The image with the rough surface shows marks left by the cutting tool. These marks are considered as chatter marks where the critical depth of cut in chatter is determined. Chatter marks are identified up to 34,000 rev/min except at 24,000, 26,000–29,000 and 32,000 rev/min. The chatter marks between 10,000 and 20,000 were easier to identify compared to the marks for spindle speeds above 20,000 rev/min.

Fig. 15 shows comparison between the predicted stability lobes and the experimentally obtained stability limits using SEM inspection for spindle speeds at which chatter marks are identified. It can be seen that some correlations between predicted and experimentally obtained results are observed. High depths of cut

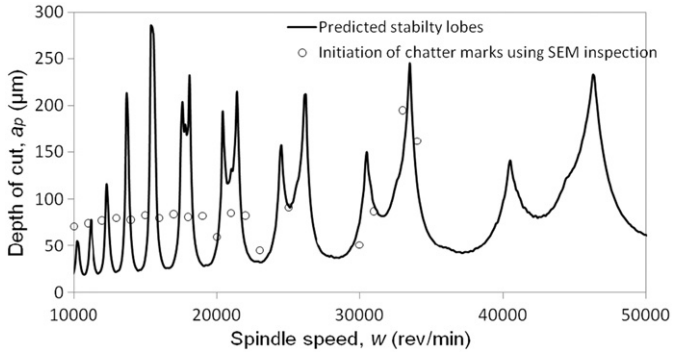

Fig. 15. Stability lobes obtained theoretically and experimentally using SEM inspection at 4 μm/tooth feed rate.

can be achieved at spindle speeds of 13.7, 15.5, 18, 21, 25–26, 31–34 and 41–47 krpm. It needs to be mentioned that the developed chatter model considers the velocity dependent cutting forces, which affect the process stability. This can be seen by the predicted higher depths of cut at stable cutting for higher spindle speeds due to the fact that the cutting forces decrease by increasing the cutting velocity. It has been also observed that initiations of burr formation begin at the same depths of cut where the chatter marks are identified. Overall, the experimental methodology conducted in this study for AISI 4340 steel can be used for identification of chatter in micro-milling. Furthermore, other experimental programmes can be also employed for further investigation and validation of the proposed theoretical chatter model. For example, acoustic emission sensors [10] or a combination of multiple sensors [9] can be considered for further validation of the model.

7. Run-out effect on the stability lobes

The influence of run-out effect on the stability lobes is investigated in this section since the run-out has a major influence on micro-milling [15]. Twelve cases at run-out angle $\gamma_0=45^\circ$ and run-out lengths $R_o=0$, 0.5 and 1 μm are investigated for four reed rates of 1, 4, 8 and 12 μm/tooth. Generally, no run-out occurs at $R_o=0$. The run-out has more significant influence at small feed rates. For example, at 1 μm/tooth feed rate with $\gamma_0=45^\circ$ and $R_o=0.5$ μm, tooth 1 cuts a maximum uncut chip thickness (h_{max}) of 1.71 μm while h_{max} for tooth 2 is 0.29 μm. For the same feed rate at $\gamma_0=45^\circ$ and $R_o=1$ μm, tooth 2 is not in contact with the workpiece material where only tooth 1 performs the cutting. Fig. 16 shows the stability lobes obtained at 8 μm/tooth feed rate with $\gamma_0=45^\circ$ and $R_o=0$, 0.5 and 1 μm in the spindle speed range between 5000 and 100,000 rev/min. For better presentation of the stability lobes at small spindle speeds, an enlarged figure is also shown. It can be seen that by increasing R_o the stability lobes move in the spindle speed axis and the stability limits decrease. The same stability lobe moves are also observed at 1, 4 and 12 μm/tooth feed rates.

The stability area ($A_{stability}$) located in the stable cutting region is used to assess the run-out and feed rate effects on the process stability. The stability area defined beneath the stability lobes is given by

$$A_{stability} = \int_{w_1}^{w_2} f(w,a_p)dw \tag{21}$$

The function $f(w,a_p)$ represents the stability lobes. The stability area is defined by integrating Eq. (21) numerically using the trapezoidal rule in the range $w_1=5000$ rev/min and $w_2=100{,}000$ rev/min.

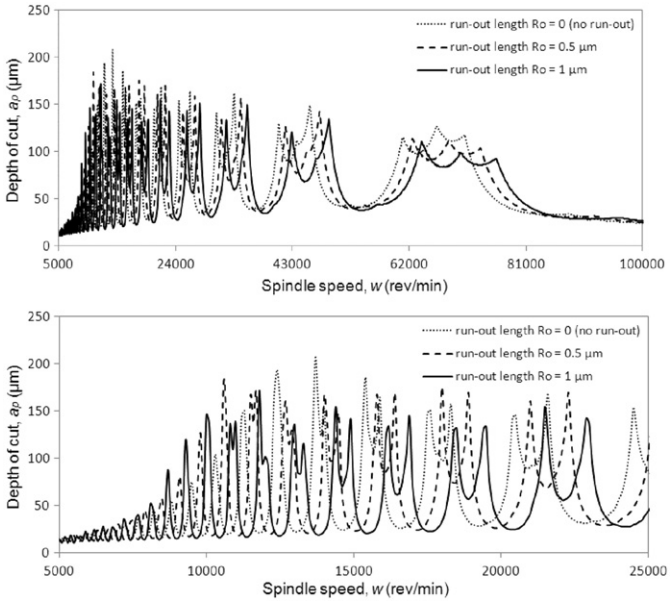

Fig. 16. Run-out effect on the stability lobs at 8 μm/tooth feed rate.

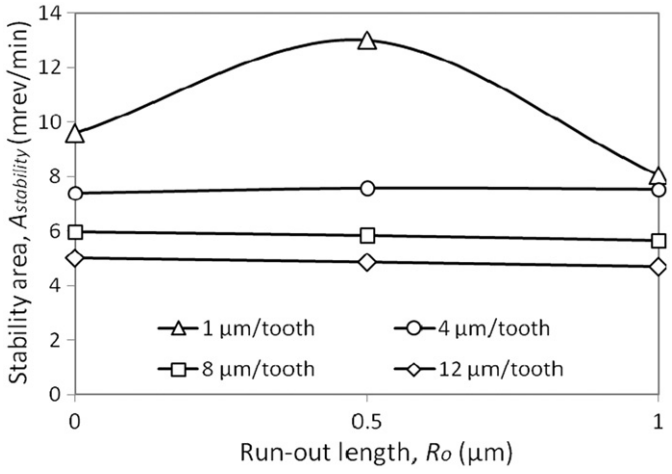

Fig. 17. Stability area at different feed rates and run-out lengths.

The stability area obtained for twelve cases is shown in Fig. 17. As expected, the stability area decreases by increasing the feed rate for all run-out lengths. This can be explained by the fact that the cutting forces increase with increasing feed rate. The stability area decreases linearly by increasing the run-out length at 8 and 12 μm/tooth while the stability area is nearly constant at 4 μm/tooth with the highest stability area at $R_o=0.5$ μm. The stability area decreases by increasing the run-out length because one of the teeth removes a higher volume of material where higher displacements and statistical variances are determined. It can be seen that at 1 μm/tooth feed rate, the effect of the run-out length shows nonlinear behaviour with the largest stability area at R_o of 0.5 μm. The large stability area at $R_o=0.5$ μm can be explained with the larger force area for the interval of one revolution-per-tool. This can be further explained with the maximum resultant forces. For example, at 1 μm/tooth feed rate with $\gamma_0=45^\circ$ and $R_o=0.5$ μm, tooth 1 cuts a maximum uncut chip thickness (h_{max}) of 1.71 μm, while h_{max} for tooth 2 is 0.29 μm. At 1 μm/tooth and no run-out ($R_o=0$) the maximum cutting forces calculated from Eq. (11) at velocity of 1571 mm/s are $F_c=8.7$ N, $F_t=7.1$ N, and the resultant force is $F_r=11.3$ N for teeth 1 and 2 or 22.6 N in total. Now, considering the run-out effect at h_{max} of 1.71 μm the $F_c=10.5$ N, $F_t=7.5$ and $F_r=12.9$ N, while at h_{max} of 0.2.9 μm the $F_c=6.2$ N, $F_t=6.5$ and $F_r=8.9$ N. The total maximum resultant forces for the case with $R_o=0.5$ μm is 21.8 N, which is smaller compared to the case with no run-out ($R_o=0$). Generally, lower forces generate a larger stability area. The constant behaviour at 4 μm/tooth feed rate is also related to the change of the cutting force due to the run-out effect. As expected, the stability area is lower at 1 μm/tooth and $R_o=1$ μm due to material removal with only one of the teeth. Since the run-out plays an important role in micro-milling, the developed chatter model can be used for identifying stable cutting conditions for different measured run-out parameters for achieving high material removal rate, low wear and good surface quality.

8. Conclusions

1. A new micro-milling chatter model has been developed and presented. The model considers the nonlinearities of the cutting forces caused mainly by the run-out phenomenon, cutting tool edge radius and cutting velocity.
2. The predicted stability limits have shown that the modal dynamic parameters have a significant influence on the stability lobes in micro-milling especially at spindle speeds higher than 35,000 rev/min.
3. To validate the micro-milling chatter model, an experimental methodology has been developed to inspect the surface finish for chatter marks in micro-milling at different spindle speeds and depths of cut using an inclined surface where the depth of cut gradually increases. Good correlations between predicted and experimentally obtained results have been observed for spindle speeds up to 32,000 rev/min.
4. The effect of the run-out was investigated at different feed rates. It has been observed that by increasing the run-out length the stability lobes move in the spindle speed axis and the stability area decreases. Also, the results have shown that by increasing the feed rate the stability area decreases due to the higher cutting forces. The stability areas at 4 and 8 μm/tooth feed rates decreased linearly by increasing the run-out length.

Based on the conducted study, the following recommendations for future work can be made: (i) determination of the micro-end mills dynamics using existing and by developing new methods, (ii) enhancement of Eq. 11 to incorporate information for the cutting tool (e.g. edge radius and rake angle), (iii) development of new experimental programmes for chatter detection in micro-milling using multi-sensors and (iv) incorporating the contact damping effect in the micro-milling chatter model in order to consider the increasing contact length due to wear and enlargement of the edge radius.

Acknowledgements

The authors wish to acknowledge the Nottingham Innovative Manufacturing Research Centre (NIMRC) and the Engineering and Physical Sciences Research Council (EPSRC) for their financial support of the work.

References

[1] Y. Altintas, G. Stepan, D. Merdol, Z. Dombovari, Chatter stability of milling in frequency and discrete time domain, CIRP—Journal of Manufacturing Science and Technology 1 (2008) 35–44.
[2] Y. Altintas, E. Budak, Analytical prediction of stability lobes in milling, CIRP Annals—Manufacturing Technology 44 (1995) 357–362.

[3] E. Budak, Y. Altintas, Analitycal prediction of chatter stability conditions for multi-degree of systems in milling, part 1—modelling; part 2—applications, Transactions of ASME Journal of Dynamic Systems Measurement and Control 120 (1998) 22–30.
[4] T. Insperger, G. Stepan, Stability of the milling process, Periodica Polytechnica 44 (2000) 47–57.
[5] T. Insperger, G. Stepan, Updated semi-discretization method for periodic delay-deferential equations with discrete delay, International Journal for Numerical Methods in Engineering 61 (2004) 117–141.
[6] E. Govekar, J. Gradisek, M. Kalveram, T. Insperger, K. Weinert, G. Stepan, I. Grabec, On stability and dynamics of milling at small radial immersion, CIRP Annals—Manufacturing Technology 54 (2005) 357–362.
[7] N.D. Sims, B. Mann, S. Huyanan, Analytical prediction of chatter stability for variable pitch and variable helix milling tools, Journal of Sound and Vibration 317 (2008) 664–686.
[8] G. Quintana, J. Ciurana, D. Teixidor, A new experimental methodology for identification of stability lobes diagram in milling operations, International Journal of Machine Tools & Manufacture 48 (2008) 1637–1645.
[9] E. Kuljanic, M. Sortino, G. Totis, Multisensor approaches for chatter detection in milling, Journal of Sound and Vibration 312 (2008) 672–693.
[10] R. Rahnama, M. Sajjadi, S.S. Park, Chatter suppression in micro end milling with process damping, Journal of Materials Processing Technology 209 (2009) 5766–5776.
[11] S.A. Tobias, W. Fishwick, The chatter of latte tools under orthogonal cutting conditions, Transaction of the ASME 80 (1958) 1079–1088.
[12] H. Opitz, Investigation and calculation of the chatter behaviour of lathes and milling machines, CIRP Annals 18 (1969) 335–342.
[13] J. Tlusty, Analysis of the state of research in cutting dynamics, CIRP Annals 27 (1978) 583–589.
[14] N.D. Sims, G. Manson, B. Mann, Fuzzy stability analysis of regenerative chatter in milling, Journal of Sound and Vibration 329 (2010) 1025–1041.
[15] S.M. Afazov, S.M. Ratchev, J. Segal, Modelling and simulation of micro-milling cutting forces, Journal of Materials Processing Technology 210 (2010) 2154–2162.
[16] M. Malekian, S. Park, M. Jun, Modelling of dynamic micro-milling cutting forces, International Journal of Machine Tools & Manufacture 49 (2009) 586–598.
[17] S.M. Afazov, S.M. Ratchev, J. Segal, Prediction and experimental validation of micro-milling cutting forces of AISI H13 stainless steel at hardness between 35 and 60 HRC, International Journal of Advanced Manufacturing Technology (2011). doi:10.1007/s00170-011-3864-7.
[18] S.M. Afazov, S.M. Ratchev, J. Segal, Determination of cutting forces and process stability in micro-milling of Ti6Al4V alloy by considering the size-effect phenomenon, Micro and NanoSystems 3 (2011) 199–209.
[19] X. Jin, Y. Altintas, Prediction of micro-milling forces with finite element method, Journal of Materials Processing Technology (2011). doi:10.1016/j.jmatprotec.2011.05.020.
[20] W.Y. Bao, I.N. Tansel, Modelling micro-end-milling operations. Part II: tool run-out, International Journal of Machine Tools & Manufacture 40 (2000) 2175–2192.
[21] ABAQUS, Theory and Analysis User's Manual, 2008, Version 6.8-13.
[22] O.C. Zienkiewicz, R.L. Taylor, The Finite Element Method for Solids and Structural Mechanics, 6th edition, Butterworth-Heinemann, Oxford, UK, 2005.
[23] S. Afazov, S. Ratchev, J. Segal, Effects of the cutting tool edge radius on the stability lobes in micro-milling, Advanced Materials Research 223 (2011) 859–868.
[24] D.J. Ewins, Modal Testing: Theory, Practice and Application, 2nd edition, Research Studies Press, Baldock, Hertfordshire, England, 2000.
[25] T. Schmitz, K. Smith, Machining Dynamics, Springer Science, LLC, New York, 2009.
[26] H. William, S.A. Teukolsky, W.T. Vetterling, B.P. Flannery, Numerical Recipes in C++: The Art of Scientific Computing, 2nd edition, Cambridge University Press, Cambridge, UK, 2002.
[27] T. Schmitz, Chatter recognition by a statistical evaluation of the synchronously sampled audio signal, Journal of Sound and Vibration 262 (2003) 721–730.
[28] I. Miller, J. Freund, Probability and Statistics for Engineers, Prentice Hall, Englewood Cliffs, New Jersey, 1985. (pp. 332–379).
[29] L. Zhongqun, L. Qiang, Solutions and analysis of chatter stability for end milling in the time-domain, Chinese Journal of Aeronautics 21 (2008) 169–178.